

## Effective isoscalar $M1$ operator determined in a study of $^{14}\text{N}^\dagger$

W. L. Sievers\*

*Cowley County Community College, Arkansas City, Kansas 67005*

J. A. Pintar,‡ R. L. Boudrie, F. W. Prosser, Jr., and Paul Goldhammer

*Department of Physics, University of Kansas, Lawrence, Kansas 66045*

(Received 8 March 1976)

The  $\gamma$ -ray decays of the 9.17-MeV state in  $^{14}\text{N}$  have been remeasured with a Ge(Li) detector. The primary purpose was to obtain an improved value of the  $M1$  decay strength of the  $(2^+, 0)$  7.03-MeV state in  $^{14}\text{N}$ . Additional information about the branching ratios and mixing ratios of other states and transitions was also obtained and is tabulated. The measured value of the  $E2/M1$  mixing of the 7.03-MeV  $\rightarrow$  0-MeV transition was  $0.74 \pm 0.09$ ; this was combined with previous measurements of this ratio and of the branching ratio and total width of the 7.03-MeV state to obtain an  $M1$  transition strength of  $(86 \pm 9) \times 10^{-3}$  eV. This strength is then compared with the predictions of various shell model calculations. This analysis suggests the introduction of an effective isoscalar magnetic dipole operator, which is constructed by fitting the ground state magnetic moment of  $^{14}\text{N}$ , as well as the 7.03-MeV  $\rightarrow$  0-MeV transition. This effective operator is then employed to predict the ground state magnetic moments of other nuclei in the  $0p$  and  $0s$  shells, with reasonable success.

NUCLEAR STRUCTURE  $^{13}\text{C}(p, \gamma)$ ,  $E = 1.75$  MeV; measured  $\sigma(\theta)$ , relative intensities; deduced  $\delta(7.03 \rightarrow 0)$ ,  $|\langle M1 \rangle|^2(7.03 \rightarrow 0)$ , other  $\delta$ 's, branching ratios.  
Enriched target. Shell model effective magnetic moment operator.

### I. INTRODUCTION

Considerable attention has been given in the literature to the low-lying states of  $^{14}\text{N}$  that appear to be reasonably well described by the  $0s^4 0d^{10}$  configuration.<sup>1</sup> Varma and Goldhammer<sup>2</sup> have emphasized that the  $M1$  strength of the 7.03-MeV  $\rightarrow$  0-MeV transition is of particular importance, since the 7.03-MeV state is uniquely characterized as  $^3D_2$  within the above configuration. Therefore, there is a need for a more accurate value of this transition strength than was available in the literature<sup>3</sup> at the time of these studies.<sup>1,2</sup>

A description of the remeasurement of the transition strength is given in Sec. II. In the course of this measurement, new values were obtained for the branching ratios of the 9.17- and 6.44-MeV states and for several mixing ratios for transitions from these states. The experimental results are given in Sec. III. The improved determination of the 7.03-MeV  $\rightarrow$  0-MeV transition strength is compared to the prediction of various shell model calculations in Sec. IV. In order to maintain agreement between theory and experiment, an effective  $M1$  operator is introduced. This effective operator is then applied to other nuclei in the  $0p$  and  $0s$  shells.

### II. EXPERIMENTAL PROCEDURES AND ANALYSIS

#### A. Procedure

Earlier measurements of the mixing ratio of the 7.03-MeV  $\rightarrow$  0-MeV transition in  $^{14}\text{N}$  have had to contend with one of two major sources of experimental uncertainty; poor statistics in coincidence experiments<sup>4,5</sup> or large, energy-dependent backgrounds.<sup>6,7</sup> The present experiment is a repetition of that in Ref. 6, i.e., measurement of the angular distribution of the  $\gamma$  rays in the  $^{13}\text{C}(p, \gamma)^{14}\text{N}$  reaction at  $E_p = 1.75$  MeV, except that the spectra were obtained with a Ge(Li), rather than a NaI(Tl), detector. With this change, the peaks in the spectra corresponding to the transitions of interest were well resolved and the Compton background from the dominant 9.17-MeV  $\rightarrow$  0-MeV transition, while still strong, was essentially flat and featureless in the regions of interest. Portions of a typical spectrum are shown in Fig. 1.

Targets of  $^{13}\text{C}$  were prepared by cracking  $\text{CH}_3\text{I}$ , enriched to 90% in  $^{13}\text{C}$ , onto 0.13-mm Au blanks. These were soldered to 1.6-mm thick brass disks, thinned to 0.98 mm over the area covered by the Au, which formed the back wall of the target chamber. This back wall was set at a  $45^\circ$  angle to the beam so that differential absorption of  $\gamma$

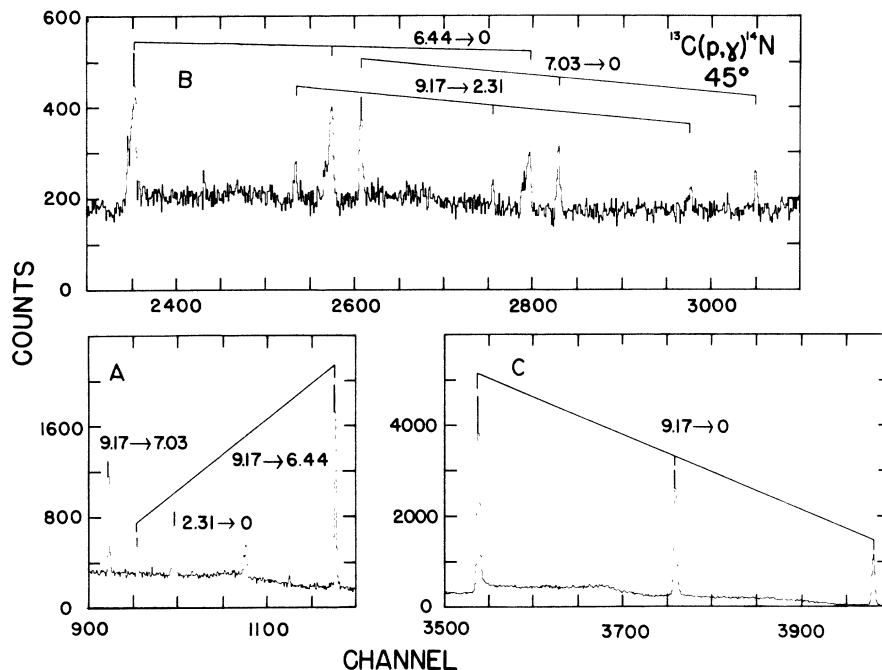


FIG. 1. Selected portions of a typical spectrum. Peaks corresponding to the transitions used in the angular distribution analysis are labeled. The width and shape of the peaks in the 6.44-MeV  $\rightarrow$ 0-MeV transition are caused by the relatively long lifetime of the 6.44-MeV state (0.63 psec, Ref. 3).

rays in the backing was minimized over the angular range of  $0^\circ$  to  $90^\circ$ . The target used to obtain the data presented here has a thickness of 7 keV for 1.75-MeV protons. Water cooling on the rear wall was used to reduce target deterioration. The final  $\sim 2$  m of the beam line was isolated from the rest of the vacuum system by a liquid nitrogen cold trap and a vacuum of  $\sim 2 \times 10^{-6}$  Torr was maintained by an ionization pump to minimize carbon buildup on the target.

A 60-cm<sup>3</sup> coaxial Ge(Li) detector was mounted on a movable arm of a goniometer, with its front face 12.1 cm from the target. A NaI(Tl) detector was placed at  $90^\circ$  on the opposite side of the chamber to monitor for beam and target changes. Standard modular electronics were used and pulses from the Ge(Li) and NaI(Tl) detectors were analyzed and stored in 4096-channel (ND161) and 1024-channel (HP5400) analyzers, respectively.

Beams of protons were accelerated to an energy of  $\sim 1.76$  MeV by the University of Kansas 4-MeV Van de Graaf accelerator. Beam currents were kept to about 4  $\mu$ A to minimize target deterioration and to reduce analyzer dead time. The  $0^\circ$  to  $90^\circ$  angular range was covered in a back and forth set of five angles and the sequence was repeated four times for a total of 20 runs, with

each run taken for an accumulated charge of 20 mC. The two spectra from each run were transferred to an on-line IBM 1800 computer and stored on magnetic tape.

The yields from the peaks in the spectra were obtained by subtraction of the background, determined by a quadratic fit to the background from a region of the spectrum on both sides of each peak and summations over the remaining counts in the peak. The peaks used in the analysis of the seven transitions of importance to the angular distribution analysis are indicated in Fig. 1. The 2.31-MeV ( $0^+$ )  $\rightarrow$ 0-MeV transition was not used in the angular distribution analysis, but was used to check the isotropy of the system. These yields were corrected for absorption in the target and backing, for monitor counts, and for dead time in both monitor and Ge(Li) detectors. These dead times varied only from 2% to 6%, so relative corrections were small. The use of monitor detector spectra with digital windows set off-line, rather than a single channel window, reduced error from gain changes in the monitor system. After all corrections were made, the yields from the several peaks for each transition and from the four passes at each angle were summed to provide the input data for the angular distribution analysis.

## B. Analysis

The spins and parities of the states at 0, 2.31, 6.44, 7.03, and 9.17 MeV, which were used in the analysis, are well established.<sup>3</sup> Therefore, no attempt was made to confirm them in the present work, other than by the success of the fit using the published values.

The individual transitions, 9.17 MeV  $\rightarrow$  0 MeV and 9.17 MeV  $\rightarrow$  2.31 MeV, and cascades, 9.17 MeV  $\rightarrow$  7.03 MeV  $\rightarrow$  0 MeV and 9.17 MeV  $\rightarrow$  6.44 MeV  $\rightarrow$  0 MeV, were first analyzed separately in least squares fits to the substate populations  $P(0)$  and  $P(1)$  of the  $J^\pi = 2^+$ , 9.17-MeV state.<sup>8</sup> In all cases,

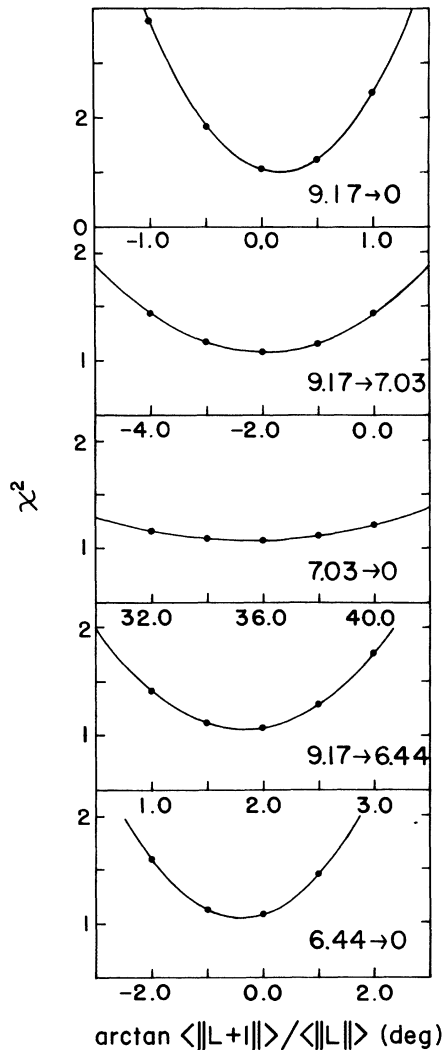


FIG. 2. Slices along each axis of the  $\chi^2$  surface generated in a simultaneous linear least squares fit, as described in the text. The mixing for the top four graphs is  $E2/M1$  and, for the bottom graph,  $M3/E2$ . The curves are quadratic fits to the points to guide the eye.

the mixing parameters agreed well with earlier values,<sup>6</sup> and satisfactory best fits were found with  $P(1)/P(0) \approx 0.2$ .

Next, a simultaneous linear least squares fit to all four cases was made by a search over the five-dimensional mixing parameter surface in the vicinity of the individual minima. A satisfactory minimum of  $\chi^2 = 1.07$  was found at  $P(1)/P(0) = 0.188 \pm 0.013$ . Projections along each axis in the vicinity of the minimum are shown in Fig. 2. The solid curves are quadratic fits to the points to guide the eye.

The final step was a nonlinear least squares fit to 12 variables. The initial values of the five mixing parameters, of the six values of  $P(0)$ , and of  $P(1)/P(0)$ , were taken from the best fit of the preceding linear fit. The values obtained for the mixing parameters are listed in Table I. The final value of  $P(1)/P(0)$  was  $0.212 \pm 0.007$  and of  $\chi^2$  was 0.92. The experimental angular distributions and the final best fits to them are shown in Fig. 3.

## III. EXPERIMENTAL RESULTS

In addition to the six transitions used in the angular distribution analysis, a number of other transitions in  $^{14}\text{N}$  were observed in the spectra. These were in general agreement with the known decays of the lower states in  $^{14}\text{N}^3$ ; however, only the 9.17- and 6.44-MeV states were populated with sufficient intensity to determine useful branching ratios for their decays.

The relative intensity of each observed transition was determined by the coefficient of  $P_0(\cos\theta)$  in a least squares fit to an expansion in even-order Legendre polynomials. The results are listed in Table II and compared to previous results. The agreement is generally good. The only exceptions are the 9.17-MeV  $\rightarrow$  0-MeV transition, where the difference is primarily a result of the reduction in the upper limits set on possible but unobserved transitions, and the 6.44-MeV  $\rightarrow$  5.83-MeV transition which is observed here with greater relative intensity than the previous upper limits. If this latter transition is pure  $E1$ , its strength is  $(4.3 \pm 0.8) \times 10^{-4}$  W.u. (Weisskopf units), a reasonable value for an isospin forbidden transition.

These branching ratios, and that of Ref. 3 for the 7.03-MeV state, were combined with the level widths calculated from Ref. 3 to obtain the partial widths for the six transitions used in the angular distribution analysis. These and the observed mixing ratios were used to calculate the partial widths for each multipole in each transition. The results are shown in Table I.

TABLE I. Mixing ratios and partial  $\gamma$ -ray decay widths for transitions in  $^{14}\text{N}$ . The partial widths for each transition were calculated from the branching ratios determined in the present work for the 9.17- and 6.44-MeV states and from Ref. 3 for the 7.03-MeV state. The partial widths for each multipole are given in Weisskopf units.

Transition	Mixing ratio	Multipoles	$\Gamma_\gamma^a$ (eV)	$\Gamma_\gamma(L)$ (W.u.) <sup>b</sup>	$\Gamma_\gamma(L+1)$ (W.u.) <sup>b</sup>
9.17 $\rightarrow$ 0	$-0.003 \pm 0.003$	( $E2/M1$ )	$7.7 \pm 0.9$	$0.47 \pm 0.06$	$<0.003$
9.17 $\rightarrow$ 2.31	0	( $E2$ )	$0.077 \pm 0.011$	$3.1 \pm 0.4$	
9.17 $\rightarrow$ 6.44	$0.031 \pm 0.006$	( $E2/M1$ )	$0.80 \pm 0.12$	$1.9 \pm 0.3$	$3.1 \pm 1.3$
9.17 $\rightarrow$ 7.03	$-0.037 \pm 0.015$	( $E2/M1$ )	$0.29 \pm 0.04$	$1.4 \pm 0.2$	$5.4^{+6.6}_{-3.8}$
7.03 $\rightarrow$ 0	$0.74 \pm 0.09$	( $E2/M1$ )	$0.124 \pm 0.012$	$0.0109 \pm 0.0014$	$1.6 \pm 0.3$
6.44 $\rightarrow$ 0	$-0.004 \pm 0.010$	( $M3/E2$ )	$(7.4 \pm 0.7) \times 10^{-4}$	$0.041 \pm 0.004$	$<1.4$

<sup>a</sup> Reference 3, corrected for the branching ratio of the 7.03-MeV state.

<sup>b</sup> Reference 9.

The present measurement of the mixing ratio for the 7.03-MeV  $\rightarrow$  0-MeV transition is compared with previous ones in Table III. The failure of the present experiment to obtain a significantly smaller error was disappointing, but was pre-saged by the shallow minimum in  $\chi^2$  for this transition shown in Fig. 2. The good agreement among the five measurements is pleasing, however, and their weighted average should be a valid number. Their agreement is further illustrated by the fact that the internal error of their average, based on the squared residuals, is smaller than the external error, based on the estimated standard deviations.

With this value for the mixing ratio and the partial width for this decay from Table I, the best

values for the multipole strengths are  $\langle ||M1|| \rangle^2 = (86 \pm 9) \times 10^{-3}$  eV or  $0.0117 \pm 0.0012$  W.u. and  $\langle ||E2|| \rangle^2 = (38 \pm 5) \times 10^{-3}$  eV or  $1.35 \pm 0.16$  W.u.<sup>9</sup> Further reduction in the assigned errors will require remeasurement of the lifetime of the 7.03-MeV state.

#### IV. THEORETICAL CONSIDERATIONS

The experimental data available in  $^{14}\text{N}$  presents an interesting opportunity for an exercise with the shell model. The reason is that the shell model wave function for a few critical states in this nucleus appear to be quite well determined.

Several authors<sup>10-13</sup> have performed shell model calculations for  $^{14}\text{N}$ , assuming just two active holes in the  $0p$  shell. In this approximation, the ground state ( $J=1$ ,  $T=0$ ) may be written as the linear combination

$$|10\rangle = A_S |^3S_1\rangle + A_P |^1P_1\rangle + A_D |^3D_1\rangle, \quad (4.1)$$

the excited state at 2.31 MeV ( $J=0$ ,  $T=1$ ) is

$$|01\rangle = B_S |^1S_0\rangle + B_P |^3P_0\rangle, \quad (4.2)$$

while the 7.03-MeV ( $J=2$ ,  $T=0$ ) level is uniquely given as

$$|20\rangle = |^3D_2\rangle. \quad (4.3)$$

The unambiguous shell model assignment in the last case provides a powerful foothold in this problem.

A second advantage is found in the simple nature of the *isoscalar* portion of the nuclear magnetic moment operator:

$$\vec{\mu}(T=0) = \frac{1}{2}\vec{J} + 0.38\vec{S}. \quad (4.4)$$

$\vec{J}$  is the total nuclear angular momentum operator, and  $\vec{S}$  the net spin. Since  $J$  is a good quantum number in nuclear states, the first term in Eq. (4.4) affects magnetic moments but not  $M1$  transitions.

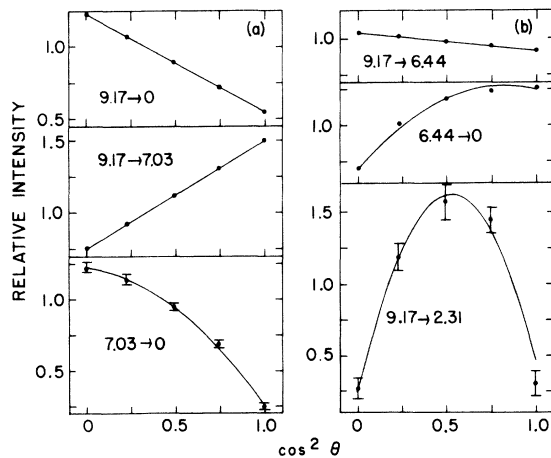


FIG. 3. Experimental angular distributions for the six transitions used in the least squares analysis. The curves are the best fits to each distribution from the simultaneous nonlinear least squares fit, as described in the text. Where error bars are not shown, the error is less than or equal to the size of the point.

TABLE II. Branching ratios for the decays of the 9.17-, 7.03-, and 6.44-MeV states in  $^{14}\text{N}$ .

$E_i$ (MeV)	$J_i^\pi; T_i^a$	$E_f$ (MeV)	$J_f^\pi; T_f$	Branching ratio	
				Present (%)	Previous <sup>a</sup> (%)
9.17	$2^+; 1$	0.0	$1^+; 0$	$85.1 \pm 1.0$	$79 \pm 4$
		2.31	$0^+; 1$	$0.85 \pm 0.08$	$1.1 \pm 0.4$
		3.95	$1^+; 0$	$<0.2$	
		4.91	$(0, 1)^-; 0$	$<0.2$	
		5.11	$2^-; 0$	$<0.2$	$<1$
		5.69	$1^-; 0$	$0.49 \pm 0.10$	$<6$
		5.83	$3^-; 0$	$0.61 \pm 0.08$	$3 \pm 2$
		6.20	$1^+; 0$	$<0.2$	
		6.44	$3^+; 0$	$8.8 \pm 0.8$	$\left. \begin{array}{l} 8 \pm 2 \\ 6.3 \pm 0.5 \end{array} \right\}$
		7.03	$2^+; 0$	$3.2 \pm 0.3$	$\left. \begin{array}{l} 3 \pm 1 \\ 3.5 \pm 0.5 \end{array} \right\}$
		7.97	$2^-; 0$	$<0.03$	
		8.06	$1^-; 1$	$<0.03$	
		8.49	$4^-; 0$	$<0.03$	
8.62	$0^+; 1$	$<0.03$			
7.03	$2^+; 0$	0.0	$1^+; 0$	$96 \pm 4$	$98.6 \pm 0.3$
		2.31	$0^+; 1$	$<3$	$0.5 \pm 0.1$
		3.95	$1^+; 0$	$<3^b$	$0.9 \pm 0.25$
6.44	$3^+; 0$	0.0	$1^+; 0$	$69.6 \pm 1.5$	$73.1 \pm 1.5$
		3.95	$1^+; 0$	$19.6 \pm 1.0$	$18.9 \pm 0.9$
		4.91	$(0, 1)^-; 0$	$<0.4$	
		5.11	$2^-; 0$	$6.4 \pm 0.6$	$6.8 \pm 0.6$
		5.69	$1^-; 0$	$<0.3$	
5.83	$3^-; 0$	$3.7 \pm 0.6$	$<3, <2, <1$		

<sup>a</sup> Reference 3.<sup>b</sup> Present, but observable only at some angles.

The  $M1$  transition  $|20\rangle \rightarrow |10\rangle$  then involves only the  ${}^3D_1$  amplitude in Eq. (4.1), since

$$\langle {}^3S_1 | \tilde{S} | {}^3D_2 \rangle = \langle {}^1P_1 | \tilde{S} | {}^3D_2 \rangle = 0. \quad (4.5)$$

Evaluating  $\langle {}^3D_1 | \tilde{S} | {}^3D_2 \rangle$ , one obtains<sup>2</sup>

TABLE III. Measured values of  $\langle ||E2|| \rangle / \langle ||M1|| \rangle$  for the 7.03-MeV  $\rightarrow$  0-MeV transition in  $^{14}\text{N}$ . The symbol  $\langle ||XL|| \rangle$  represents the reduced matrix element for  $XL$  multipole radiation. The mean is the weighted mean of the five values and its error is the weighted internal error. The external error is 0.050.

Reference	Value	Method
Gorodetsky <i>et al.</i> , Ref. 4	$0.6 \pm 0.2$	$^{12}\text{C}({}^3\text{He}, p\gamma)$
Gallmann <i>et al.</i> , Ref. 5	$0.7 \pm 0.1$	$^{12}\text{C}({}^3\text{He}, p\gamma)$
Prosser <i>et al.</i> , Ref. 6	$0.6 \pm 0.1$	$^{13}\text{C}(p, \gamma)$
Swann, Ref. 7	$0.6 \pm 0.15$	$^{14}\text{N}(\gamma, \gamma)$
Present work	$0.74 \pm 0.09$	$^{13}\text{C}(p, \gamma)$
Mean	$0.669 \pm 0.031$	

$$\Gamma_{M1}(7.03 \rightarrow 0) = 0.126 |A_D|^2, \quad (4.6)$$

where the width  $\Gamma$  is in eV. Using the experimental value of  $\Gamma$  obtained above one has

$$|A_D|^2 = 0.68 \pm 0.07. \quad (4.7)$$

The magnitude of the remaining amplitudes in Eq. (4.1) can be found from the experimental value for the ground state magnetic moment

$$\begin{aligned} \langle \mu \rangle &= 0.88 |A_S|^2 + 0.50 |A_P|^2 + 0.31 |A_D|^2 \\ &= 0.404, \end{aligned} \quad (4.8)$$

and the normalization condition

$$|A_S|^2 + |A_P|^2 + |A_D|^2 = 1. \quad (4.9)$$

We find

$$|A_S|^2 = 0.09 \pm 0.04, \quad (4.7')$$

$$|A_P|^2 = 0.23 \mp 0.11. \quad (4.7'')$$

It will also be useful to find  $|B_S|^2$  and  $|B_P|^2$ . The  $|01\rangle$  state has well known isospin analogs in  $^{14}\text{C}$  and  $^{14}\text{O}$ , which display unusually large  $ft$  values in their  $\beta$  decay to the  $^{14}\text{N}$  ground state for an

allowed transition. For practical purposes the Gamow-Teller matrix element can be set equal to zero, yielding the condition

$$\sqrt{3} A_s B_s + A_p B_p \approx 0. \quad (4.10)$$

Equations (4.10), (4.7'), and (4.7'') and the normalization  $|B_s|^2 + |B_p|^2 = 1$  yield

$$|B_p|^2 = 0.53 \pm 0.21, \quad (4.10')$$

$$|B_s|^2 = 0.47 \mp 0.21. \quad (4.10'')$$

The magnitudes of these amplitudes derived in a variety of shell model calculations are displayed in Table IV, to be compared with the values obtained in the "fit" given above. The comparison is very poor in that the fit values are quite different from those obtained in shell model calculations.

First, note that there is excellent agreement among the shell model calculations in that the ground state is very near  $LS$  coupling with  $0.90 \leq |A_D|^2 \leq 0.96$ . The fit value for  $|A_D|^2$  is substantially less. There is also consensus in the shell model work that  $|B_s|^2 > |B_p|^2$ . This is important because it is a consequence of the fact that the  $^1S_0$  partial wave of the effective interaction is much more attractive than the  $^3P_0$  partial wave. The amplitudes of the fit are compatible with that fact only near the extremity of the error bars. Furthermore, at that extremity one would have a minimum value for  $|A_D|^2$  (0.61) and a value for  $|A_P|^2$  (0.34) more than four times in excess of any shell model calculation.

The most disturbing feature of the comparison is that the values obtained in the fit lie closer to  $jj$  coupling than to the shell model values. If the shell model work is of any use at all, it should distinguish between  $LS$  and  $jj$  coupling.

The standard tactic in this type of problem is to introduce an effective moment operator.<sup>14</sup> In this example, it is particularly easy. Equation (4.4) is modified into

$$\vec{\mu}(T=0) = \frac{1}{2} \lambda \vec{J} + 0.38 \gamma \vec{S}, \quad (4.11)$$

with the introduction of two parameters  $\lambda$  and  $\gamma$ , which are both unity for the bare operator. This is the most general form the isoscalar part of the magnetic dipole operator can take on, so long as one retains its single particle character.

One can then fit  $\lambda$  and  $\gamma$  to two bits of data; the magnetic dipole moment of  $^{14}\text{N}$  of Eq. (4.8), and the width of the magnetic dipole transition in Eq. (4.6). The values of  $|A_L|^2$  are taken directly from the shell model calculation, and the results are displayed in Table V. It is also of interest to express these parameters in terms of the orbital ( $g_{IP} + g_{IN}$ ) and spin ( $g_{SP} + g_{SN}$ ) factors for the proton and neutron:

$$(g_{IP} + g_{IN})' = \lambda, \quad (4.12)$$

$$(g_{SP} + g_{SN})' = \gamma (g_{SP} + g_{SN}) + (\lambda - 1). \quad (4.13)$$

The prime denotes an "effective" operator.

The value of  $\gamma$  appears to be quite well determined, showing little sensitivity to the shell model wave function used. This is because  $\gamma$  depends only on  $A_D$ :

$$\gamma = (0.823 \pm 0.042) A_D^{-1}, \quad (4.14)$$

on which the shell model calculations are in consensus. Regrettably,  $\lambda$  is not so well fixed because  $\lambda$  depends on  $A_s$ :

$$\lambda = 0.808 + 0.38 \gamma [ |A_D|^2 - 2 |A_s|^2 ]. \quad (4.15)$$

The shell model work indicates that  $|A_s|^2$  is very small, and consequently hard to determine pre-

TABLE IV. Values of  $|A_L|^2$  and  $|B_L|^2$  from Eqs. (4.1) and (4.2), as found in various calculations.

Reference	$ A_D ^2$	$ A_s ^2$	$ A_p ^2$	$ B_s ^2$	$ B_p ^2$
Cohen and Kurath I <sup>a</sup>	0.92	0.01	0.07	0.75	0.25
Cohen and Kurath II <sup>b</sup>	0.92	0.02	0.06	0.78	0.22
Elliot and Flowers	0.96	0.01	0.03	0.65	0.35
Norton and Goldhammer <sup>c</sup>	0.90	0.09	0.01	0.62	0.38
$jj$ coupling <sup>d</sup>	0.74	0.04	0.22	0.33	0.67
Eqs. (4.7), (4.10'), and (4.10'')	$0.68 \pm 0.07$	$0.09 \pm 0.04$	$0.23 \mp 0.11$	$0.47 \mp 0.21$	$0.53 \pm 0.21$

<sup>a</sup> This is the (8-16) 2 BME fit of Ref. 10 with  $\epsilon = 5.67$  MeV, as shown in Ref. 1.

<sup>b</sup> This is the (8-16) 2 BME fit of Ref. 10 with  $\epsilon = 5.15$  MeV, as shown in Ref. 1.

<sup>c</sup> This is the 4 BME fit of Ref. 13.

<sup>d</sup> The  $jj$  coupled wave functions displayed assume a pure  $p_{1/2}^{-2}$  configuration.

TABLE V. Parameters of the effective magnetic dipole operator using the shell model wave functions of Table IV.

Reference	$\gamma$	$\lambda$	$\frac{1}{2}(g'_{Sp} + g'_{SN})$
Bare operator	1.0	1.0	0.88
Cohen and Kurath I	$0.85 \pm 0.04$	$1.10 \pm 0.01$	$0.80 \pm 0.04$
Cohen and Kurath II	$0.85 \pm 0.04$	$1.09 \pm 0.01$	$0.79 \pm 0.04$
Elliott and Flowers	$0.84 \pm 0.04$	$1.11 \pm 0.01$	$0.78 \pm 0.04$
Norton and Goldhammer	$0.87 \pm 0.04$	$1.04 \pm 0.01$	$0.78 \pm 0.04$

cisely.

Table VI is the result of an investigation to find if the effective  $M1$  operator has any further validity. Since we have only the isoscalar term, applications are limited. Ground state static moments can be done directly if  $T=0$ . In addition, if both  $M1$  moments are known for a pair of mirror nuclei, the sum of these moments depends only on the isoscalar component of the operator. Several such cases are displayed in Table VI, where we compare results with the bare operator and the effective operator to the experimental value. We have used only the  $0p$  shell wave functions of Norton and Goldhammer in Table VI, because they are conveniently available. Consistency thereby dictated use of the effective moment operator determined by the same fit in  $^{14}\text{N}$ .

Results are encouraging. The effective operator yields improvement over the bare operator for  $A=6, 13,$  and  $15$ . In  $A=10$  and  $11$ , a comparatively large correction to the bare operator is needed, and the effective operator used provides a comparatively small one (in the wrong direction). It may be significant that in all of the states investigated except the ground states of the  $A=10$  and  $11$  systems  $LS$  coupling is a reasonably good approximation. In  $^{10}\text{B}$  and  $^{11}\text{C}$

no  $LS$  state contributes as much as 50% to the total wave function. The poorest example of  $LS$  coupling elsewhere is in  $A=13$ , where the  $^2P$  state of optimal orbital symmetry accounts for 72% of the wave function. Perhaps it is not surprising that an effective operator fitted to  $LS$  wave functions works well only in  $LS$  coupling.

That brings us to the problem of the derivation of the effective moment operator. How do the corrections arise? There are two categories of possibilities: (1) The effective operator incorporates mixing of configurations from higher shells. (2) The magnetic moment is simply modified in the presence of other nucleons, by relativistic effects, meson exchange effects, or velocity dependent nuclear forces.

In an attempt to determine which effect is important here, we have used the effective operator to calculate the magnetic moment of  $^2\text{H}$ , and the  $^3\text{H} + ^3\text{He}$  mirror pair. The spirit of using an effective operator dictates that one neglect configuration mixing. One then assumes that  $^2\text{H}$  is pure  $^3S_1$  and that  $^3\text{H}$  and  $^3\text{He}$  are pure  $^2S_{1/2}$ . The results appear in the final two entries of Table VI, and, surprisingly, the agreement with experiment is excellent.

Of course, we know that the deuteron does

TABLE VI. Ground state magnetic dipole moments in nuclear magnetons (using the  $0p$  shell wave functions of Norton and Goldhammer) found with the bare operator, and the effective operator with  $\lambda=1.04 \pm 0.01$ ,  $\gamma=0.87 \pm 0.04$ .

Nucleus	$\mu$	$\mu$	$\mu$
	Bare operator	Effective operator	Experiment
$^6\text{Li}$ ( $J=1$ )	0.87	$0.84 \pm 0.02$	0.822
$^{10}\text{B}$ ( $J=3$ )	1.87	$1.88 \pm 0.03$	1.8007
$^{11}\text{B} + ^{11}\text{C}$ ( $J=\frac{3}{2}$ )	1.78	$1.80 \pm 0.03$	1.66
$^{13}\text{C} + ^{13}\text{N}$ ( $J=\frac{1}{2}$ )	0.35	$0.39 \pm 0.01$	0.3803
$^{15}\text{N} + ^{15}\text{O}$ ( $J=\frac{1}{2}$ )	0.37	$0.41 \pm 0.01$	0.4358
$^2\text{H}$ ( $J=1$ )	0.88	$0.85 \pm 0.02$	0.857
$^3\text{H} + ^3\text{He}$ ( $J=\frac{1}{2}$ )	0.88	$0.85 \pm 0.02$	0.851

possess a  ${}^3D_1$  component. Consequently, we conclude that the effective operator must, at least in part, absorb the mixing of the  ${}^3D_1$  amplitude. The admixture of  ${}^3D_1$  component needed to fit the magnetic moment with the bare single nucleon operator is 3.9%. The actual admixture of the  ${}^3D_1$  component is generally thought<sup>15</sup> to be nearer 7%. Therefore, it is likely that the effective operator also corrects for some sort of modification of the bare nucleon  $M1$  operator.

The interesting point is that the effective isoscalar operator determined above yields reasonable results in both the  $0p$  and  $0s$  shell nuclei, so long as the wave function is reasonably represented by  $LS$  coupling.

It is worthwhile noting in Table VI that the experimental value of the magnetic moment of the deuteron ( $0.857\mu_N$ ) is very nearly equal to the experimental value of the sum of the moments for  ${}^3H + {}^3He$  ( $0.851\mu_N$ ). These two numbers would be precisely the same if our effective operator were exactly valid. As it stands the effective operator appears to be a reasonable approximation.

Further applications are warranted if one has sufficient experimental data and reliable shell model wave functions.  $T=0 \rightarrow T=0$   $M1$  transitions

are an obvious target. We have made a cursory survey in the  $0p$  shell and found no viable candidates worth reporting in detail. Let us give just one example to illustrate the difficulties. A likely looking candidate is the 3.95-MeV  $\rightarrow$  0-MeV ( $JT=10 \rightarrow 10$ ) transition in  ${}^{14}N$ . The  $M1$  width is reasonably determined to be  $(0.58 \pm 0.12) \times 10^{-3}$  eV. The Cohen and Kurath I fit yields a width of  $0.408 \times 10^{-3}$  eV, while the II fit yields  $1.321 \times 10^{-3}$  eV. The effective moment operator would worsen agreement considerably in the first case, and help substantially in the second. To make a discriminating statement on the merit of using the effective operator one must be able to choose between the two sets of wave functions. This is difficult as the overlap integrals between the sets are 0.999. Quite evidently the  $T$  forbidden  $M1$  transitions are frequently very sensitive to the precise shell model wave functions employed. The simplicity and lack of ambiguity found in the 7.03-MeV  $\rightarrow$  0-MeV transition investigated in this paper is a singular stroke of good fortune.

The use of computational facilities at Argonne National Laboratory for a portion of the data analysis is gratefully acknowledged.

†Work supported in part by the U.S. Atomic Energy Commission, The National Science Foundation, and The General Research Fund of the University of Kansas.

\*Present address: Northern Oklahoma College, Tonkawa, Oklahoma 74653.

‡Present address: Phillips Petroleum, Bartlesville, Oklahoma.

<sup>1</sup>H. J. Rose, O. Häusser, and E. K. Warburton, *Rev. Mod. Phys.* **40**, 591 (1968).

<sup>2</sup>S. Varma and P. Goldhammer, *Nucl. Phys.* **A125**, 193 (1969).

<sup>3</sup>F. Ajzenberg-Selove, *Nucl. Phys.* **A152**, 1 (1970).

<sup>4</sup>S. Gorodetsky, R. M. Freeman, A. Gallmann, and F. Haas, *Phys. Rev.* **149**, 801 (1966).

<sup>5</sup>A. Gallmann, F. Haas, and B. Heusch, *Phys. Rev.* **164**, 1257 (1967).

<sup>6</sup>F. W. Prosser, Jr., R. W. Krone, and J. J. Singh,

*Phys. Rev.* **129**, 1716 (1963).

<sup>7</sup>C. P. Swann, *Phys. Rev.* **148**, 1119 (1966).

<sup>8</sup>Since the spins of both target and projectile are  $\frac{1}{2}$ , only the  $m=0$  and  $\pm 1$  substates can be populated in this reaction.

<sup>9</sup>D. H. Wilkinson, in *Nuclear Spectroscopy*, edited by F. Ajzenberg-Selove (Academic, New York, 1960), Part B, Chap. V.

<sup>10</sup>S. Cohen and D. Kurath, *Nucl. Phys.* **73**, 1 (1965).

<sup>11</sup>P. Goldhammer, J. R. Hill, and J. Nachamkin, *Nucl. Phys.* **A106**, 62 (1967).

<sup>12</sup>J. P. Elliott and B. H. Flowers, *Proc. Roy. Soc. Lond.* **A229**, 536 (1955).

<sup>13</sup>J. L. Norton and P. Goldhammer, *Nucl. Phys.* **A165**, 33 (1971).

<sup>14</sup>A. de-Shalit and I. Talmi, *Nuclear Shell Theory* (Academic, New York and London, 1963).

<sup>15</sup>P. Goldhammer, *Rev. Mod. Phys.* **35**, 40 (1963).